

Table S1 MRI sequences and acquisition for pregnant women

Center	Sequences	TR/TE (ms)	FOV (mm)	Matrix	Slice thickness (mm)	Slice gap (mm)	Fat suppression	Flip angle (°)
Center 1	T2WI-Haste	1,000/85	370×384	256×224	5	1	No	150
	T2WI-True FISP	3.5/1.6	379×400	256×224	5	1	No	60
	T1WI-FLASH	125/2.43	389×382	256×224	5	1	No	70
Center 2	T2WI-Haste	1,100/87	400×400	320×320	5	1	No	80
	T2WI-True FISP	3.6/1.8	379×400	256×256	5	1	No	70

MRI, magnetic resonance imaging; TR, repetition time; TE, echo time; FOV, field of view; T2WI, T2-weighted imaging; T1WI, T1-weighted imaging; FISP, fast imaging with steady-state free precession; FLASH, fast low-angle shot.

Table S2 Reader's evaluation agreement and disagreement

MRI morphological findings	Agreement	Disagreement	Disagreement ratio
Placenta previa subtype	119	6	4.8%
Main location of placental attachment	117	8	6.4%
Location of intraplacental dark T2 bands	112	13	10.4%
Placental heterogeneity	115	10	8.0%
Intervertebral cervical canal	117	8	6.4%
Uterine/placental bulge	110	15	12.0%
Intraplacental dark T2 bands	112	13	10.4%
Loss of low T2 retroplacental line	114	11	8.8%
Myometrial thinning/disruption	115	10	8.0%
Bladder wall interruption	115	10	8.0%
Focal exophytic placental mass	124	1	0.8%

Table S3 MRI morphological findings evaluation and readers agreement

MRI morphological findings	0	1	2	Kappa	95% CI
Placenta previa subtype	Normal or low lying	Incomplete	Complete	0.894	0.812–0.976
Main location of placental attachment	Front walls	Back walls	Both front and back walls	0.882	0.802–0.962
Location of intraplacental dark T2 bands	Normal	Upper uterine segment	Lower uterine segment	0.770	0.654–0.886
Placental heterogeneity	Inexistent	Suspicious	Clear	0.758	0.593–0.879
Placental tissue protrusion into the cervical canal	Inexistent	Suspicious	Clear	0.758	0.599–0.917
Uterine/placental bulge	Inexistent	Suspicious	Clear	0.721	0.598–0.844
Intraplacental dark T2 bands	Inexistent	Suspicious	Clear	0.758	0.640–0.876
Loss of low T2 retroplacental line	Inexistent	Suspicious	Clear	0.786	0.668–0.904
Myometrial thinning/disruption	Inexistent	Suspicious	Clear	0.783	0.658–0.908
Bladder wall interruption	Inexistent	Suspicious	Clear	0.787	0.667–0.907
Focal exophytic placental mass	Inexistent	Suspicious	Clear	0.906	0.724–0.990

MRI, magnetic resonance imaging; CI, confidence interval.

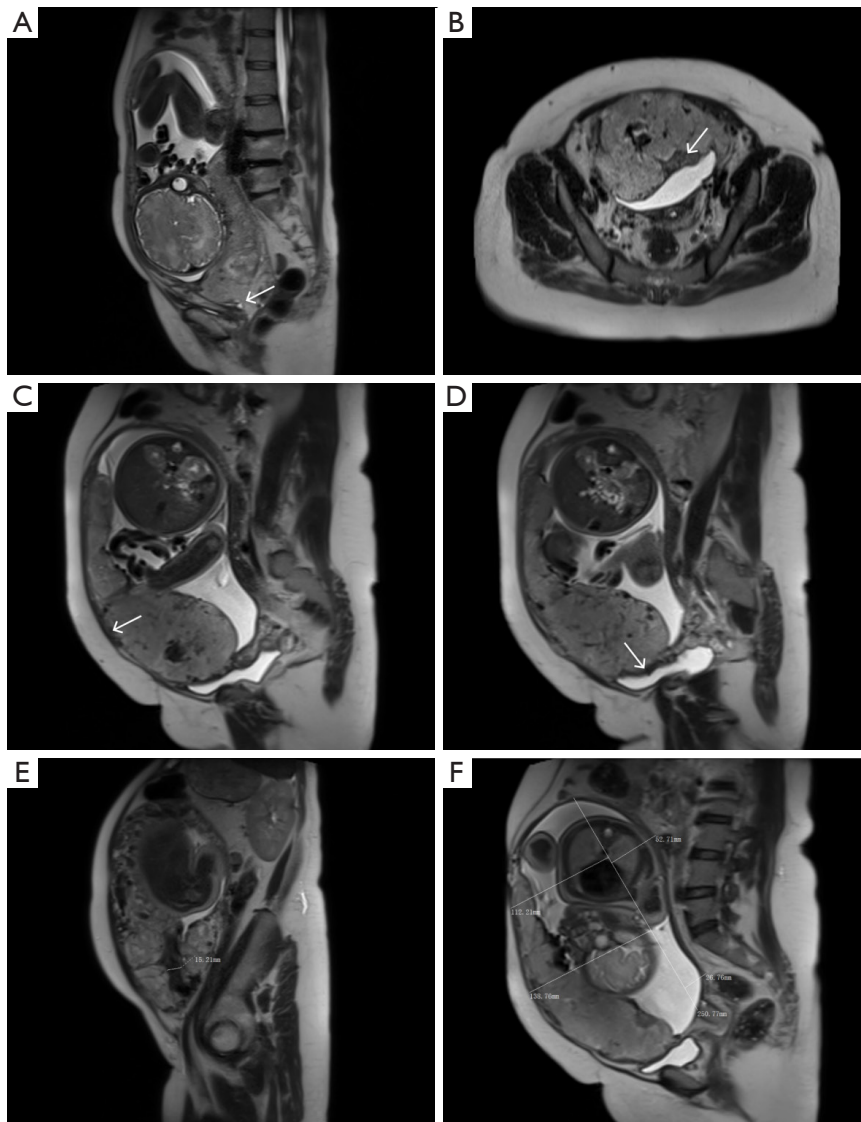


Figure S1 Illustrative figures presenting MRI morphological findings or anatomical indicators. (A) Placental tissue protrusion into the cervical canal, as indicated by the white arrows in the figure. (B) Intraplacental dark T2 bands, as indicated by the white arrows in the figure. (C) Loss of low T2 retroplacental line, as indicated by the white arrows in the figure. (D) Bladder wall interruption, as indicated by the white arrows in the figure. (E) The diameter of placental abnormal vasculature. There is evidence of proliferative blood vessels within the placental tissue, with a measured diameter of 15.21 mm. (F) The ratio of uterine anteroposterior diameter. A straight line was drawn on the sagittal T2-weighted image, connecting the internal os of the cervix to the highest point of the uterine fundus. The anterior-posterior diameters of the upper and lower segments of the uterus were measured perpendicular to this line, and the ratio between the 2 measurements was used to determine the degree of lower segment bulging. A ratio less than 1 indicates lower segment bulging. In the case indicated by the dashed line in the diagram, the ratio between the anterior-posterior diameters of the upper (164.92) and lower (165.52) segments of the uterus was 0.99, indicating diffuse lower segment bulging. MRI, magnetic resonance imaging.

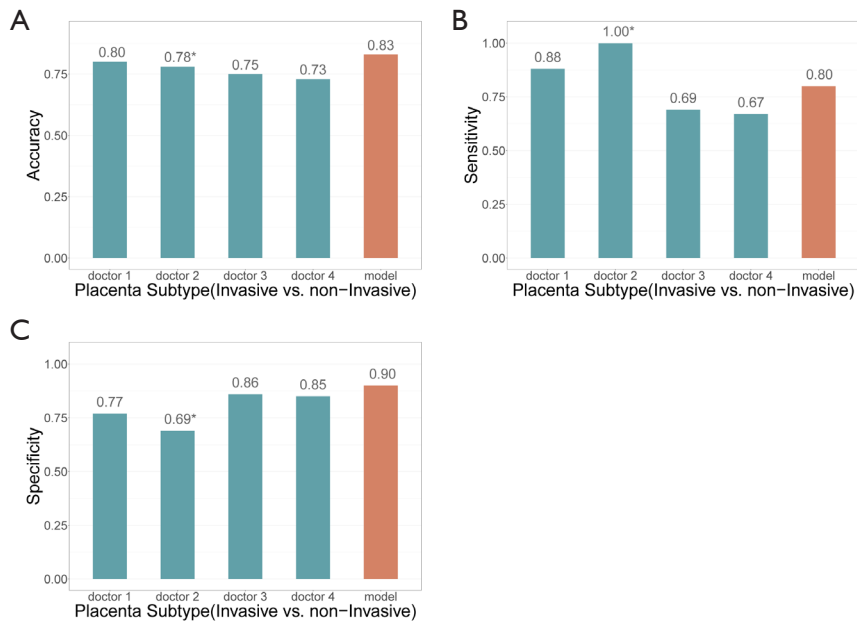


Figure S2 Predictive performances of 4 radiologists and proposal model in the external cohort (40 cases). The McNemar test was utilized to evaluate the disparities between the diagnostic outcomes of the four radiology experts and the model, with a significance level of $P < 0.05$ denoting a notable distinction. The statistically significant findings are denoted by an asterisk (*). The accuracy (A), sensitivity (B), and specificity (C) of the 4 radiologists were compared to our model in placenta subtype (invasive *vs.* non-invasive).

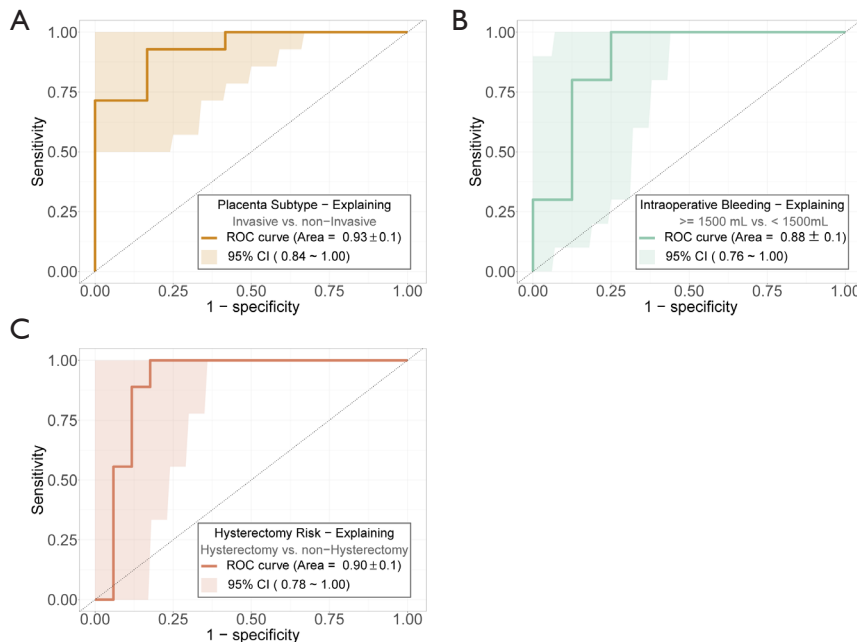


Figure S3 The performance of retrained model after feature selection was on a par with the performance of proposed model in placenta subtype, intraoperative bleeding, and hysterectomy risk. (A) The AUROC of placenta subtype (invasive *vs.* non-invasive) at retrained model after feature selection. (B) The AUROC of intraoperative bleeding ($\geq 1,500$ *vs.* $< 1,500$ mL) at retrained model after feature selection. (C) The AUROC of hysterectomy risk (hysterectomy *vs.* non-hysterectomy) at retrained model after feature selection. ROC, receiver operating characteristic; AUROC, area under the receiver operating characteristic; CI, confidence interval.